

Noncollinear Polarization Gating of Attosecond Pulse Trains in the Relativistic Regime

M. Yeung,^{1,*} J. Bierbach,^{1,2} E. Eckner,^{1,2} S. Rykovanov,¹ S. Kuschel,^{1,2} A. Sävert,^{1,2} M. Förster,² C. Rödel,^{1,2,3}
G. G. Paulus,^{1,2} S. Cousens,⁴ M. Coughlan,⁴ B. Dromey,⁴ and M. Zepf^{1,2,4,†}

¹*Helmholtz-Institut Jena, Fröbelstieg 3, 07743 Jena, Germany*

²*Friedrich-Schiller-Universität Jena, Max-Wien-Platz 1, 07743 Jena, Germany*

³*SLAC National Accelerator Laboratory, 2575 Sand Hill Road, Menlo Park, California 94025, USA*

⁴*Department of Physics and Astronomy, Queen's University Belfast, BT7 1NN, United Kingdom*

(Received 27 May 2015; published 4 November 2015)

High order harmonics generated at relativistic intensities have long been recognized as a route to the most powerful extreme ultraviolet pulses. Reliably generating isolated attosecond pulses requires gating to only a single dominant optical cycle, but techniques developed for lower power lasers have not been readily transferable. We present a novel method to temporally gate attosecond pulse trains by combining noncollinear and polarization gating. This scheme uses a split beam configuration which allows pulse gating to be implemented at the high beam fluence typical of multi-TW to PW class laser systems. Scalings for the gate width demonstrate that isolated attosecond pulses are possible even for modest pulse durations achievable for existing and planned future ultrashort high-power laser systems. Experimental results demonstrating the spectral effects of temporal gating on harmonic spectra generated by a relativistic laser plasma interaction are shown.

DOI: 10.1103/PhysRevLett.115.193903

PACS numbers: 42.65.Ky, 52.27.Ny, 52.35.Mw

High-power laser interactions with plasma surfaces at intensities sufficient to drive electron oscillations with peak velocities close to the speed of light can lead to the generation of bright attosecond pulses in the reflected beam [1]. In the relativistically oscillating mirror model (ROM) [2,3], this attosecond radiation is a result of Doppler up-shifting of the incident laser to extreme ultraviolet wavelengths due to the motion of the reflecting surface. Filtering out the low order components from the broad spectrum that is generated results in a pulse with attosecond scale duration. Another generation mechanism that is efficient for very steep plasma density gradients is coherent wake emission (CWE) [4], which involves the coupling of plasma oscillations in the preplasma density ramp into electromagnetic waves and is hence limited to frequencies less than the plasma frequency.

For oblique incidence interactions, this radiation is emitted in a pulse train with a period of one laser cycle (half a cycle for normal incidence), which is observed in the spectral domain as high order harmonics of the laser frequency; however, for application of these sources to time-resolved measurements, isolation of a single pulse is preferred. One approach is to simply use a shorter duration driving pulse [5]; however, at the high powers required for relativistic interactions, such single cycle laser systems are not currently available. Alternatively, a number of techniques exist that can gate the generation process for multicycle pulses. These methods include the attosecond lighthouse [6,7], noncollinear optical gating [8], and polarization gating [9,10].

Techniques such as polarization gating have generally not been considered experimentally possible for ultraintense lasers and ROM harmonics to date (although some theoretical studies have been made [10,11]), as the nonlinear phase

(B integral) in the multiple transmissive optics used for gating high harmonic generation (HHG) in gaseous media with smaller lasers would have led to substantial pulse distortion. Although, in principle, larger beam diameters can be used to reduce the intensity and mitigate B -integral issues, this quickly becomes expensive and impractical as beam diameters become tens of centimeters or larger; hence, alternative techniques with fewer transmissive optics would be invaluable. Here we present a new method which combines two gating approaches—noncollinear and polarization gating—in an elegant setup requiring minimal transmissive optics allowing the application of polarization gating on high-power laser systems for the first time. We present results from a proof of principle experiment applying this technique to ROM harmonics providing the first experimental observation of temporal gating of a relativistic high HHG process. This is a critical step towards reaching high brightness isolated attosecond pulses suitable for use as both pump and probe in studies of atomic and molecular electron dynamics.

Consider two circularly polarized parallel noncollinear laser pulse replicas with opposite handedness and a controlled delay. When focused, these beams will overlap spatially allowing their fields to interfere leading to linear polarization at the point of temporal overlap where the pulses have similar intensity. For driving mechanisms that are suppressed by elliptically polarized pulses (such as HHG in gaseous media [12] and normal incidence solid interactions [3,13]), this gates the attosecond emission to the period when the laser polarization is linear. In addition to this polarization gating effect, because the two pulses are noncollinear, the resultant wave vector varies from one beam direction to the other over the period of temporal

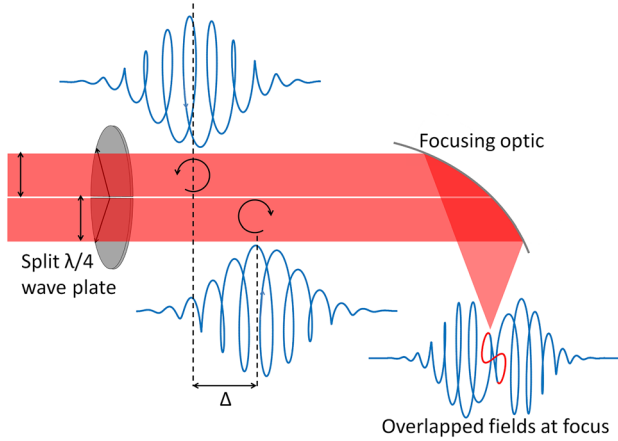


FIG. 1 (color online). Sketch of the noncollinear polarization gating method. A split quarter wave plate with orthogonal optical axes converts two delayed linearly polarized half beam pulses into left and right circularly polarized pulses. These pulses overlap at focus and create a linear gate.

overlap. Hence, the attosecond pulses, which follow the wave vector of the resultant driving field, have a time-dependent direction.

Because of the aforementioned B -integral issues, beam splitters are not suitable for generating the pulse replicas in ultrahigh intensity systems; however, a simple solution is to replace one mirror before the focusing optic with a mirror split into two halves with controllable position on one half. Then this field can be synthesized by the use of a quarter wave plate split in two halves and set so that the optical axes are orthogonal leading to circular pulses with opposite handedness (see Fig. 1 for a sketch).

The coupling of the two gating effects can be represented by an angle-dependent gating function $G(\theta, t) = G_{\text{NC}}(\theta, t)G_{\text{PG}}(t)$, where $G_{\text{NC}}(\theta, t)$ is the gating term that results from the wave front rotation due to the noncollinearity of the two beams, and $G_{\text{PG}}(t)$ is the gating term that results from the polarization gating.

For the noncollinear term we need to determine the wave front angle at a given time which can be calculated by considering that the resultant wave vector is the summation of the wave vectors of each beam weighted by their respective electric field amplitudes [8,14]. The angle $\beta(t)$ that the wave front makes with the center axis for pulses with a relative delay of Δ and FWHM durations of τ (assuming Gaussian temporal profiles) is given by $\beta(t) \approx 2 \ln(2)\gamma(\Delta/\tau^2)t$ [8]. Here γ is the angle that the wave front of each half beam makes with the center axis and the approximation is valid for small γ , β , and t , where $t = 0$ is the midpoint between the two pulses. For a circular beam with a top hat spatial distribution of radius R (typical for high-power, large diameter laser systems), focused by an optic with focal length f , the wave vector of each beam half (as defined by the direction of the centroid of each beam) makes an angle $\tan(\gamma) = \pm 4R/3\pi f$ with the focal axis.

If we assume a constant divergence of Θ for each attosecond pulse, then the noncollinear gating term can be written as $G_{\text{NC}}(\theta, t) = \exp\{-2[\theta - \beta(t)]^2/\Theta^2\}$. It should be noted that, for the case of ROM harmonics, the attosecond pulse divergence is not constant but is dependent on the denting of the plasma surface which will vary over time [15,16]. However, in this case we are only concerned with a small number of consecutive pulses gated from the pulse train; hence, the divergence should not vary significantly.

The polarization gating term is given by the ellipticity dependence of the generation mechanism $G_{\text{PG}}(t) = f(\xi(t))$, where we define the ellipticity as the ratio of the minor and major axis of the electric field vector ellipse. For small t , the ellipticity $\xi(t)$ is given by [17] $\xi(t) = |2 \ln(2)(\Delta/\tau^2)t|$. Note that this is very similar to the expression for $\beta(t)$ except for the factor of γ .

Although normal incidence surface harmonic generation mechanisms are known to be strongly suppressed by elliptical polarization [3,13], the dependence of the ROM mechanism at oblique angles is not clearly understood. Experiments by Easter *et al.* [18] at 35° showed a factor of 3 reduction in the harmonic intensity for circular pulses along with a small angular deflection away from the specular direction which would further reduce the on-axis contribution. Furthermore, simulations by Rykovanov *et al.* [10] showed that the collinear polarization gating scheme can still operate at near-normal incidence angles at least up to 15° .

An experimental investigation was performed to test the ellipticity dependence of ROM harmonics at 22.5° incidence at the 30 fs, 800 nm JETI40 laser in Jena. The laser contrast is enhanced by a single plasma mirror [19] and is then focused onto fused silica targets by an $F/3$ off-axis parabola to a peak intensity of $\approx 6 \times 10^{19} \text{ W cm}^{-2}$. The reflected radiation is detected by an extreme ultraviolet spectrometer consisting of an imaging toroidal mirror and a freestanding gold transmission grating. For drawings of a similar setup and further details about the spectrometer, see Refs. [20–22].

The efficiency of the ROM process was optimized by the use of a specially coated reversed mirror placed before the final mirror in order to introduce a controlled prepulse, as was demonstrated by Kahaly *et al.* [23]. As the prepulse is moved earlier, increasing the preplasma scale length, the initial harmonic signal, which is completely dominated by CWE as is clear from the harmonic cutoff, is completely suppressed before the appearance of ROM harmonic orders [24]. This transition between mechanisms agrees with previous observations of the scale length dependence [23,26]. Thus, although some of the observed orders are below the CWE cutoff, we can attribute the emission to the ROM mechanism.

The ellipticity was varied by the use of a quarter wave plate and the results are shown in Fig. 2. In this figure, a Gaussian fit for the first 5 points given by $f(\xi) = \exp[-\ln(10)\xi^2/\xi_{\text{th}}]$ is plotted, where $\xi_{\text{th}} = 0.27$ was found to be a best fit for the threshold ellipticity, which is defined

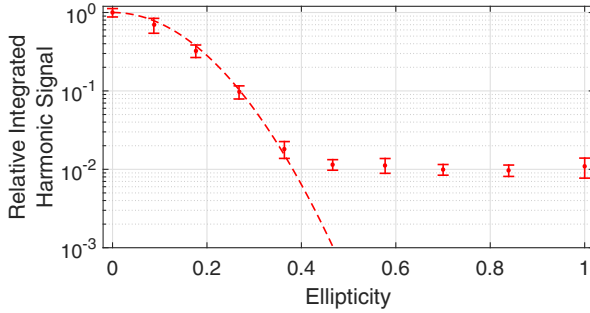


FIG. 2 (color online). Spectrometer signal integrated over harmonics 13–28 for varying laser ellipticity and plotted relative to the linear case. Each data point is an average of 20 shots and the error bars represent the standard error of the mean. The dotted line represents a fit to the first 5 data points only.

as the value for which the relative signal is 10%. The remaining points are limited by the detector sensitivity and incomplete suppression due to the non-normal incidence (only a small number of shots in each sequence contain any harmonic signal).

The gate width (defined at 10% of the maximum) for the polarization gate is given by [17] $\delta t_{\text{PG}} \approx 1.44\xi_{\text{th}}\tau^2/\Delta$, while that for the noncollinear gate can be shown to be $\delta t_{\text{NC}} \approx 1.55(\Theta/\gamma)(\tau^2/\Delta)$ [24]. Since the ellipticity dependence $f(\xi)$ can be fitted by a Gaussian, we have the following expression for the combined gate width:

$$\delta t \approx \left(\frac{\delta t_{\text{PG}}^2 \delta t_{\text{NC}}^2}{(\delta t_{\text{PG}}^2 + \delta t_{\text{NC}}^2)} \right)^{1/2}. \quad (1)$$

In Fig. 3 the delay required for a single cycle (for one pulse per cycle mechanisms like oblique incidence ROM) and half cycle (for two pulses per cycle mechanisms like HHG in gases or normal incidence ROM) gate and the corresponding reduction in the gate intensity are plotted against pulse duration for the collinear and noncollinear polarization gating schemes. The attosecond pulse divergence depends on a variety of factors, such as the laser divergence, source size reduction, and, as already mentioned, target surface denting; however, the value of 20 mrad used is consistent with other experiments using similar experimental parameters to those presented here [20,27]. It is clear that, for the measured ellipticity dependence of these relativistic harmonics, use of the noncollinear scheme can significantly relax the requirements on the delay needed to isolate a single pulse, which, in turn, allows a stronger intensity in the gated region.

An additional investigation into the use of the split beam method was conducted using the same experimental setup as for the ellipticity study, but now, instead of the full beam quarter wave plate, a custom-ordered split mica wave plate with orthogonal optical axes was used. Fine control over the delay between each half beam was achieved using two 500 μm fused silica wafers where one had adjustable

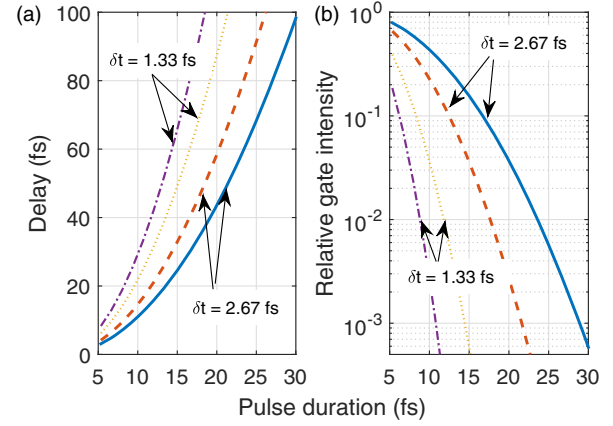


FIG. 3 (color online). (a) Delay required for a single cycle (solid and dashed lines) and half cycle (dotted and dot-dashed lines) gate for an 800 nm pulse with collinear polarization gating (dashed and dot-dashed lines) and noncollinear gating for $F/3$ focusing ($\gamma \approx 4^\circ$) and 20 mrad attosecond pulse divergence (solid and dotted lines). (b) Gate intensity relative to the intensity at zero delay between the left and right circular pulses for the same cases as (a).

rotation to increase the effective path of one half beam. Note that, in principle, these wafers can be replaced by a split translatable mirror to avoid the extra transmissive optics. The relative phase and timing between the pulses was measured by observing the polarization-dependent focal spot images.

The far-field distributions along the y axis for semi-circular beams split by the x axis are given by [28]

$$U(\theta) \propto \frac{J_1(kR \sin \theta)}{kR \sin \theta} \pm i \frac{\mathbf{H}_1(kR \sin \theta)}{kR \sin \theta}, \quad (2)$$

where J_1 and \mathbf{H}_1 are the first order Bessel function of the first kind and the first order Struve function, respectively. Here the rightmost term is positive for the half beam in the positive y space and negative for the other. For the case where the two beams are in phase, the two distributions are added and are reduced to the usual Airy focus as would be expected for the full beam. Because of the orientation of the split wave plate's axes, when one polarization is in phase across both beams, the orthogonal polarization will have phases of $\pm\pi/2$. Thus, the distributions for each beam in Eq. (2) must be multiplied by $\pm i$, and the combined function for this polarization will have a destructive minimum for $\theta = 0$.

The recorded focal spot images are shown in Fig. 4 for both P and S polarization and for 3 different delays. Additionally, lineouts for the zero delay case are plotted along with the analytical distribution from Eq. (2). Since the ROM mechanism is significantly more efficient for P polarization at oblique angles [2,3,29], the delays are always set to be integer multiples of an optical cycle to maintain a single intensity peak in the P -polarized focal

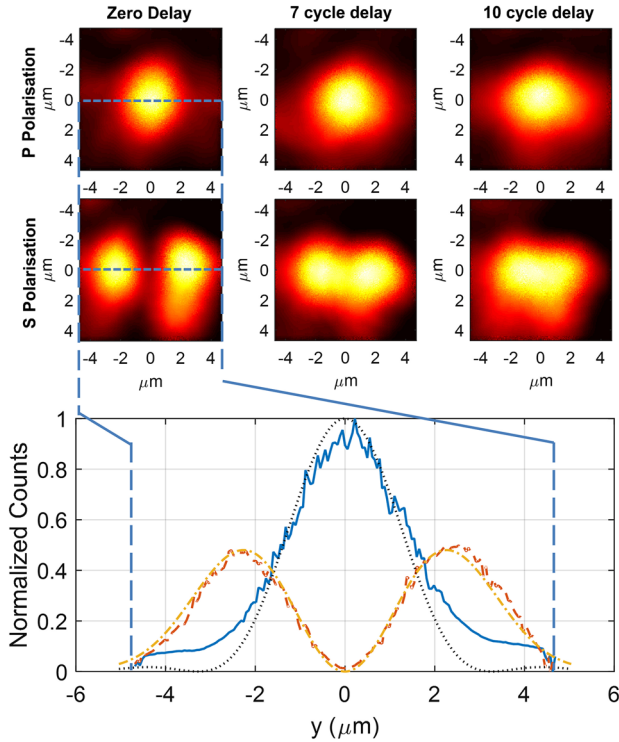


FIG. 4 (color online). Recorded focal spot images for the P -polarized (top images) and the S -polarized (bottom images) spots for delays of zero (left), 7 cycles (middle), and 10 cycles (right). Below the images, lineouts for zero delay are plotted for the P -polarized (solid line) and S -polarized (dashed line) cases as well as the analytical solution for a split circular top hat beam for P (dotted line) and S (dot-dashed line) polarization.

spot in much the same way as for normal noncollinear gating [8,14]. We also note that the two S -polarized spots will be out of phase by π so that any emission from these regions will cancel out on axis in the far field. For oblique incidence this is largely irrelevant as this contribution is negligible, but for normal incidence interactions when there is no distinction between S and P polarization, this will lead to a more complicated polarization structure in the off-axis emission, which will also be gated.

Increasing the delay between the pulses leads to a reduction in the contrast of the destructive minimum in the S -polarized case and a broadening of the spot in the direction the beams are split in the P -polarized case. This can be understood as a reduction in the time over which the two circular pulses can interfere; thus, the focal spot increasingly becomes just the summed intensities of the individual pulses. The deviation from the analytical case at the edges of the P -polarized lineout are likely due to imperfections in the split edge of the wave plate and glass wafers.

Using the split beam gating setup reduces the on-target peak intensity to $\approx 2 \times 10^{19} \text{ W cm}^{-2}$ due to losses and the splitting of the energy into S and P polarizations. For the zero-delay and gated pulse cases, a clear harmonic signal

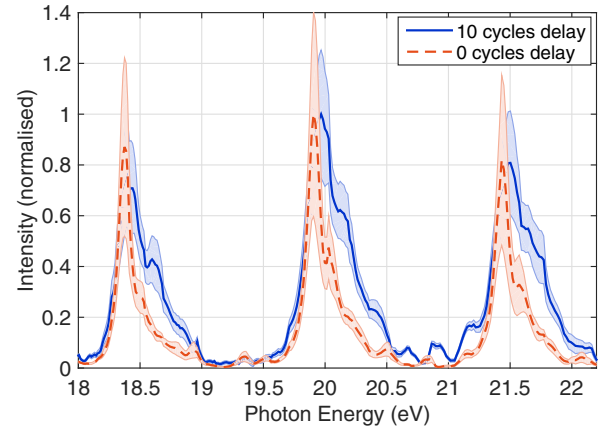


FIG. 5 (color online). Experimental high harmonic spectra averaged over 10 shots while using the split beam gating setup. The spectrum for harmonics 12–14 are shown for delays of 0 (dotted line) and 10 (solid line) cycles between the split beams and have been normalized to the zero-delay peak of the 13th harmonic. The shaded region indicates the rms signal variation.

up to the 24th and 20th harmonic, respectively, can still be seen while the spectrometer was set to observe harmonic orders as low as the 12th. Introducing a 10 cycle delay between the two half beams leads to a reduction of the integrated harmonic signal by a factor of 3.3 over the observed spectral range. Observed spectra for no delay and 10 cycles delay are shown in Fig. 5 and have been normalized in order to compare the harmonic bandwidth. For 10 cycles delay, and assuming a divergence of 20 mrad, the calculated gate width for polarization gating alone is 4.7 cycles while, when we adjust for the noncollinear term integrated between $\theta = \pm 5$ mrad (due to the acceptance angle of the imaging spectrometer), the gate width becomes 3.6 cycles. This agrees well with the measured FWHM bandwidth for the 13th harmonic, $\Delta\nu/\nu_0 = 0.236$, which would correspond to a transform limited gate of 3.4 cycles, and is significantly broader than the case with no delay, which is a clear signature of gating of the pulse train. The overall reduction in the integrated harmonic signal is also consistent with the reduction of the number of contributing cycles. At longer delays (and thus shorter gate times) the harmonic signal level is too weak to be distinguished above the background extreme ultraviolet signal.

We can discount intensity gating, where harmonics near the cutoff are broadened since only the most intense cycles contribute to their emission, because the harmonics of interest here are well below the highest observed frequency. The asymmetry of the harmonic broadening is due to the reduced intensity for the gated pulse (slightly over 50% of the ungated intensity), which results in a lower recession velocity of the surface due to the pressure of the laser. Hence, the frequency of the harmonic order in the ungated case experiences a stronger redshift [30]. The temporal dynamics of this surface denting can also lead to a femtochirp, whereby the periodicity of the emitted pulse

train varies with the instantaneous velocity of the plasma surface which can also lead to harmonic broadening [31–33]. In the Supplemental Material this effect is modeled for the current parameters and it is found that the effect is negligible for the gated case [24].

Figure 3 and the experimental results show that pulses of 30 fs duration are not suitable for achieving single cycle pulses. However, the significant spectral broadening, in good agreement with predictions, demonstrates the effectiveness of this gating scheme, and the scalings calculated here suggest that gate widths capable of isolating single pulses are possible for existing high-power laser systems such as the LWS20 [5] and future systems such as the sub-20-fs JETI200 system at the Helmholtz-Institute in Jena.

In conclusion, a novel gating scheme has been presented that employs the effect of wave front rotation from two noncollinear beams to reduce the possible gate width from polarization gating alone. This scheme can be easily scaled to very high-power, large diameter beams required for reaching the highest intensities. Experimental results clearly show the spectral signature of gating of pulse trains generated by the ROM mechanism when using this method and represent the first experimental demonstration of temporal gating for a relativistic HHG process. It is expected that experiments with shorter pulsed lasers in the near future will be able to reach single isolated pulses using this method.

This work was supported by Laserlab Europe (Grant Agreement No. 284464, ECs Seventh Framework Programme), the European Regional Development Fund (EFRE), and Deutsche Forschungsgemeinschaft (SFB TR18-A7). We acknowledge the invaluable support of F. Ronneberger and B. Beleites as laser operators. S.R. acknowledges the support by the Helmholtz Association (Young Investigator’s Group VH-NG-1037).

* Current address: Department of Physics and Astronomy, Queen’s University Belfast, BT7 1NN, United Kingdom.

† m.zepf@uni-jena.de

- [1] G. D. Tsakiris, K. Eidmann, J. Meyer-ter-Vehn, and F. Krausz, *New J. Phys.* **8**, 19 (2006).
- [2] S. V. Bulanov, N. M. Naumova, and F. Pegoraro, *Phys. Plasmas* **1**, 745 (1994).
- [3] R. Lichters, J. Meyer-ter-Vehn, and A. Pukhov, *Phys. Plasmas* **3**, 3425 (1996).
- [4] F. Quéré, C. Thaur, P. Monot, S. Doboş, Ph. Martin, J.-P. Geindre, and P. Audebert, *Phys. Rev. Lett.* **96**, 125004 (2006).

- [5] P. Heissler *et al.*, *Phys. Rev. Lett.* **108**, 235003 (2012).
- [6] H. Vincenti and F. Quéré, *Phys. Rev. Lett.* **108**, 113904 (2012).
- [7] J. A. Wheeler *et al.*, *Nat. Photonics* **6**, 829 (2012).
- [8] C. M. Heyl, S. N. Bengtsson, S. Carlström, J. Mauritsson, C. L. Arnold, and A. L’Huillier, *New J. Phys.* **16**, 052001 (2014).
- [9] P. B. Corkum, N. H. Burnett, and M. Y. Ivanov, *Opt. Lett.* **19**, 1870 (1994).
- [10] S. G. Rykovanov, M. Geissler, J. Meyer-ter-Vehn, and G. D. Tsakiris, *New J. Phys.* **10**, 025025 (2008).
- [11] T. Baeva, S. Gordienko, and A. Pukhov, *Phys. Rev. E* **74**, 065401(R) (2006).
- [12] K. S. Budil, P. Salières, A. L’Huillier, T. Ditmire, and M. D. Perry, *Phys. Rev. A* **48**, R3437 (1993).
- [13] M. Yeung *et al.*, *Phys. Rev. Lett.* **112**, 123902 (2014).
- [14] M. Louisy *et al.*, *Optica* **2**, 563 (2015).
- [15] M. Yeung, B. Dromey, D. Adams, S. Cousens, R. Hörlein, Y. Nomura, G. D. Tsakiris, and M. Zepf, *Phys. Rev. Lett.* **110**, 165002 (2013).
- [16] H. Vincenti, S. Monchocé, S. Kahaly, G. Bonnaud, Ph. Martin, and F. Quéré, *Nat. Commun.* **5**, 3403 (2014).
- [17] Z. Chang, *Phys. Rev. A* **70**, 043802 (2004).
- [18] J. H. Easter, J. A. Nees, B. X. Hou, A. Mordovanakis, G. Mourou, A. G. R. Thomas, and K. Krushelnick, *New J. Phys.* **15**, 025035 (2013).
- [19] C. Rödel, M. Heyer, M. Behmke, M. Kübel, O. Jäckel, W. Ziegler, D. Ehrt, M. C. Kaluza, and G. G. Paulus, *Appl. Phys. B* **103**, 295 (2011).
- [20] C. Rödel *et al.*, *Phys. Rev. Lett.* **109**, 125002 (2012).
- [21] S. Fuchs *et al.*, *Rev. Sci. Instrum.* **84**, 023101 (2013).
- [22] J. Jasny, U. Teubner, W. Theobald, C. Wülker, J. Bergmann, and F. P. Schäfer, *Rev. Sci. Instrum.* **65**, 1631 (1994).
- [23] S. Kahaly, S. Monchocé, H. Vincenti, T. Dzelzainis, B. Dromey, M. Zepf, Ph. Martin, and F. Quéré, *Phys. Rev. Lett.* **110**, 175001 (2013).
- [24] See Supplemental Material at <http://link.aps.org/supplemental/10.1103/PhysRevLett.115.193903>, which includes Ref. [25], for a derivation of the gate widths, data concerning the suppression of CWE, and a discussion of femtochirp effects.
- [25] C. Thaur and F. Quéré, *J. Phys. B*, **43**, 213001 (2010).
- [26] A. Tarasevitch, K. Lobov, C. Wünsche, and D. von der Linde, *Phys. Rev. Lett.* **98**, 103902 (2007).
- [27] B. Dromey *et al.*, *Nat. Phys.* **5**, 146 (2009).
- [28] A. Barna, *J. Opt. Soc. Am.* **67**, 122 (1977).
- [29] P. Gibbon, *Phys. Rev. Lett.* **76**, 50 (1996).
- [30] M. Zepf *et al.*, *Phys. Plasmas* **3**, 3242 (1996).
- [31] E. C. Welch, P. Zhang, F. Dollar, Z.-H. He, K. Krushelnick, and A. G. R. Thomas, *Phys. Plasmas* **22**, 053104 (2015).
- [32] F. Quéré, C. Thaur, J.-P. Geindre, G. Bonnaud, P. Monot, and Ph. Martin, *Phys. Rev. Lett.* **100**, 095004 (2008).
- [33] M. Behmke *et al.*, *Phys. Rev. Lett.* **106**, 185002 (2011).